

Neutron resonance spectroscopy: Argon*

H. I. Liou, J. Rainwater, G. Hacken, and U. N. Singh

Columbia University, New York, New York 10027

(Received 31 October 1974)

Results are presented of the high resolution measurements of the neutron total cross section of natural argon to 580 keV. Of the 24 levels observed in ^{40}Ar , 6 are assigned to be $l=0$, and 18 to be $l=1$. Resonance parameters were obtained using area and R -matrix analyses for s levels, and area analysis including the Doppler broadening effect for p levels. The s and p strength functions and average level spacings for ^{40}Ar were $10^4 S_0 = 0.91^{+0.77}_{-0.37}$, $10^4 S_1 = 0.33^{+0.14}_{-0.09}$, $\langle D_0 \rangle = (87^{+13}_{-11})$ keV, and $\langle D_1 \rangle = (24^{+5}_{-4})$ keV.

[NUCLEAR REACTIONS $^{40}\text{Ar}(n, n)$, (n, γ) , $E = 1\text{--}580$ keV; measured $\sigma_t(E)$;
deduced E_0 , $g\Gamma_n$, l , J , S_0 , S_1 , $\langle D_0 \rangle$, $\langle D_1 \rangle$.]

I. INTRODUCTION

This is one of a series¹⁻¹⁵ of papers reporting the results of high resolution pulsed neutron time of flight spectroscopy using the Columbia University Nevis synchrocyclotron as a source. This paper presents the measured total neutron cross section of Ar vs energy from 1 to 580 keV, and the resonance parameters for 24 observed resonances. Natural argon is almost all ^{40}Ar (99.6%), with 0.063% ^{38}Ar and 0.337% ^{36}Ar . The measured σ_t vs E is mainly due to ^{40}Ar . All the observed resonances are ^{40}Ar levels, since otherwise the peak cross sections would be much smaller. $A = 40$ is in a mass region below the ($3s$) maximum of the s strength function, and above the ($2p$) maximum of the p strength function, so there is interest in measuring its s and p strength functions. ^{40}Ar has the binding energy for an extra neutron $= 6.098$ MeV, and $I^\pi = 0^+$.

The data were obtained in a major cyclotron run from transmission measurements using our 202.05 m flight path. The 8192 detector timing channels have 25 ns width down to 54.5 keV, which covers most level structures, followed by 50 ns width to 5.9 keV, 100 ns width to 2.5 keV, and 200 ns width to 1 keV. Of the 24 levels observed below 580 keV, 6 are considered to be $l=0$, while 18 are considered to be $l=1$. In addition to the resonance energy E_0 , we obtained $(g)\Gamma_n$ values for every resonance, and J values for p resonances in 3 favorable cases. The spin statistical weight factor $g=1$ for s levels, and $=1$ or 2 for p levels, corresponding to the compound nuclear spin $J = \frac{1}{2}$ or $\frac{3}{2}$, respectively.

Early low resolution measurements¹⁶ of the total cross section vs energy for natural Ar gave $\sigma_t = 0.68$ b/atom from ~ 15 eV to 1 keV. Although ^{36}Ar is only 0.337% abundant in natural Ar, it gives

a disproportionately large contribution to the natural Ar σ_t vs E below ~ 10 keV. Chrien, Jain, and Palevsky,¹⁷ using the Brookhaven fast chopper, measured the ^{36}Ar total cross section from 0.1 eV to 6 keV and obtained $\sigma_t \approx 70$ b/atom below ~ 1 keV. They fit their results to a virtual level at (-9.8 ± 1.0) keV, with $\Gamma_n^0 = (82 \pm 10)$ eV, and $\Gamma_\gamma = 1.85 \pm 0.22$ eV. The value of Γ_γ was chosen to fit Henshaw's¹⁸ thermal capture cross section $\sigma_\gamma \approx 4$ b/atom for ^{36}Ar . Henshaw also obtained¹⁸ thermal cross sections of $\sigma_t = (77 \pm 9)$ b/atom for ^{36}Ar and $\sigma_s = 0.36$ b/atom for ^{40}Ar and 0.61 b/atom for natural Ar. Krohn and Ringo¹⁹ obtained $\sigma_s = (73.7 \pm 0.4)$ b/atom for ^{36}Ar and (0.647 ± 0.003) b/atom for natural Ar at thermal energy. McMurtrie and Crawford obtained²⁰ (6.5 ± 1.0) b/atom for the thermal capture cross section of ^{36}Ar . The latest BNL 325 recommended²¹ values for the ^{40}Ar thermal cross sections are $\sigma_\gamma = (0.660 \pm 0.010)$ b/atom, $\sigma_s = (0.40 \pm 0.02)$ b/atom, and $a_{\text{coh}} = (1.83 \pm 0.05)$ fm.

Unpublished measurements by Seibel, Bilpuch, and Newson²² were made of σ_t vs energy for natural Ar from 40 to 670 keV, with most resonances resolved. We obtained the same l assignments as they did. They analyzed four more levels above 580 keV, while we resolved four extra p levels, one at 192.8 keV and three below 60 keV.

II. EXPERIMENTAL DETAILS AND ANALYSIS PROCEDURES

The transmission measurements for argon were made at the same time that samples of the Er separated isotopes¹ and many other elements were studied. The detector system consisted of a slab of ^{10}B viewed by a bank of four NaI detectors, each having a 28 cm diam crystal. The time of flight count spectra were sorted using an on-line EMR 6050 computer with 8192 timing channels. A detailed description of the synchrocyclotron oper-

ation was given in Ref. 1.

For the measurements using natural Ar, we had a pair of 7.6 m long steel pipes having 0.38 mm thick Al end windows. One was used as a dummy with He gas and the other for the Ar. Some flushing of the Ar tank was done with Ar and it was then filled to 13.1 atm. A thorough flushing was done for the He tank which was used at atmospheric pressure. Although the supply of Ar was 99.996% pure, subsequent analysis indicated that about 5% of air remained with the Ar due to incomplete flushing of the argon tank. Measurements were made at various pressures corresponding to $(1/n) = 4.31, 13.9,$ and 45.4 b/atom of Ar. About 1 h counting time was used for each Ar pressure and for the He tank ("open") (for $T=1$ reference). This gave 7.2×10^6 total histogram counts for the thickest Ar sample, and 13×10^6 total counts for the He.

The evaluation of the proper energy and transmission sample dependent background was complicated and was made with the help of standard filter measurements in which a 0.32 cm Co filter was kept in the beam, with and without the thickest argon sample also in the beam. The standard filter method has been described in an earlier paper.⁶ The Co filter shows a transmission bottoming dip ($T \approx 0$) at 4.29 keV, as well as nearly bottoming dips at 8.06, 10.70, 16.95, and 22.52 keV. The transmission peaks on the low side of these strong dips are reduced by a factor equal to the air-argon mixture transmission when it is also present.

Initially the analysis was done assuming that only Ar was present and gave results inconsistent with other results¹⁶ that $\sigma_t \sim 0.7$ b/atom below 1 keV, but consistent with $\approx 5\%$ air mixed in the sample. After using the standard filter results to make the proper sample and energy dependent background subtractions, the resulting σ_t vs E was corrected for 5% air contamination using published σ_t vs E curves²³ for nitrogen and oxygen.

A major problem in the analysis to obtain proper transmission, cross section (T, σ) values vs energy for each sample thickness was to establish the correct sample and energy dependent background for each sample and for the "open." The strong, broad s level at 76.2 keV in ^{40}Ar was important for this purpose. It must have $\sigma_{\text{peak}} = 2.6 \times 10^6 \times (41/40)^2 \times (1 \text{ eV}/E) \text{ b/atom} = 35.9 \text{ b/atom}$. For the thick sample, it is bottoming ($T=0$), giving the thick sample background at that energy. For the medium sample, an implied $T_{\text{min}} \approx 0.07$ permits a background evaluation at that energy for the medium sample. The implied $T_{\text{min}} = 0.454$ for the thin sample there. Using nearly equal background subtractions for the thin sample and "open" measurements, the required values of these subtractions at 76.2 keV are established. A subsequent

study showed that self-consistency of the results for the different sample thicknesses was obtained if each background subtraction energy dependence had a common shape which was the same as for the nonbackground subtracted "open" count vs energy. A "smoothed" shape was used to eliminate the effects of Al in the flight path. Errors in choosing the background subtractions will cause slight shifts in the σ_t values, but will not influence the shape of σ_t vs E . The resulting σ vs E were consistent with the standard filter results.

A resonance area analysis¹ was first used to extract the level (g) Γ_n values. It includes the Doppler broadening effect for p levels, and the interference between σ_p and σ_{res} for s levels. We used $\Gamma_\gamma = 0.5 \text{ eV}$ for each level, but our resulting $g\Gamma_n$ values were in all cases insensitive to Γ_γ for $\Gamma_\gamma \lesssim 5 \text{ eV}$. The transmission dip area for each level and sample thickness implies a functional relationship between $g\Gamma_n$ and Γ for the level. Intersection of two or more $g\Gamma_n, \Gamma$ curves for different sample thicknesses yields $g\Gamma_n$ and Γ values for the level studied. We use $(g\Gamma_n)/g \approx \Gamma - 0.5 \text{ eV}$, where g is unity for s levels, and $g=1$ or 2 for p

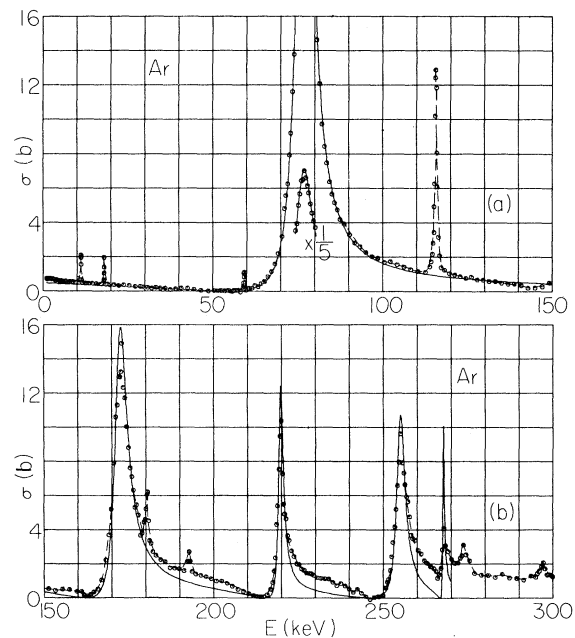


FIG. 1. (a), (b) The measured σ_t vs E for natural argon from 1 to 300 keV, using many-channel averages except at the narrow p levels. The thickest sample ($1/n = 4.31$ b/atom) results are used for $\sigma_t \lesssim 4$ b/atom, while the other two thinner sample results are used where appropriate for $\sigma_t > 4$ b/atom. The solid curves are R -matrix fits for s levels in ^{40}Ar . The dashed curves which smoothly connect the measured points are an aid to the eye for the p levels, and for some between level regions.

levels having $J = \frac{1}{2}$ or $\frac{3}{2}$, respectively. In the three cases where we could establish g (and J) for p levels, $g\Gamma_n \gg 5$ eV. For the weaker p levels, the solutions are relatively insensitive to the choice of Γ .

In addition to the area analysis, we also used R -matrix analysis for the s levels. Both results were in good agreement for the Γ_n values, but the R -matrix fit gave between-level cross sections lower than measured in some regions. This is discussed in more detail in the next section.

III. RESULTS AND DISCUSSION

Figures 1(a) and 1(b) show the measured σ_t vs E from 1 to 300 keV after correction for the air in the samples. Since, except at the narrow p levels, the data suggested that σ_t varied slowly with E compared to the channel separation, we have used many channel averages to reduce the statistical fluctuations. The thickest sample results are used for $\sigma_t \lesssim 4$ b/atom, with the two thinner samples used, where appropriate, for $\sigma_t > 4$ b/atom. One hundred and fifty channel averages were used below 10 keV, ~ 10 channel averages near 150 keV, and ≤ 5 channel averages above 200 keV. Figure 2 shows the single channel σ_t vs E behavior from 300 to 600 keV based mainly on the thickest sample results. The medium sample results were used near resonance peaks. The solid curves in Figs. 1(a) and 1(b) are R -matrix fits for s levels in ^{40}Ar . The dashed curves are an aid to the eye for the p levels, and for some between level regions where the measured σ_t is significantly above the s level fit curves. The curve in Fig. 2 just connects the measured points.

The results of the resonance parameter evaluations are given in Table I for s levels and in Table II for p levels. The levels showing interference

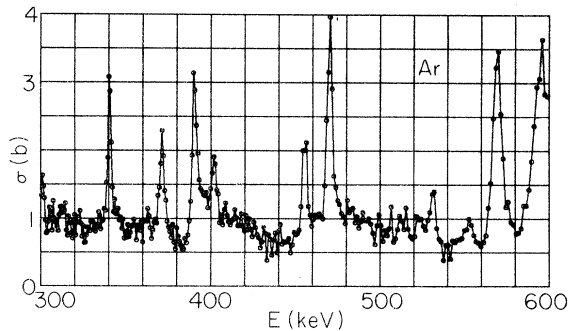


FIG. 2. The measured single channel σ_t vs E for natural argon from 300 to 600 keV based mainly on the thickest sample results, except near resonance peaks using the medium sample results. The curve just connects the experimental points.

TABLE I. Resonance parameters of ^{40}Ar for $l=0$ levels.

E_0 (keV)	Γ_n (keV)
76.2 ± 0.4	5.5 ± 0.4
171.7 ± 0.5	4.5 ± 0.4
219.4 ± 0.5	1.8 ± 0.2
254.3 ± 0.5	3.4 ± 0.4
267.6 ± 0.5	0.52 ± 0.12
390.6 ± 0.9	1.4 ± 0.3

asymmetry are assigned $l=0$; otherwise $l=1$. For p levels, we also list the level spins in three favorable cases. Our l assignments agree well with those by the Duke group.²² Recently, BNL-325 *Neutron Cross Sections*²¹ presents the weighted mean of our preliminary results and those of the Duke group for ^{40}Ar resonance parameters. Our final parameters are significantly different in many cases from those in Ref. 21.

The six analyzed $l=0$ levels are all between 70 and 400 keV. The Duke group obtained an additional s level at 596 keV, having $\Gamma = 4$ keV, which we also see. Using these seven observed $l=0$ levels, we evaluate the s strength function and average spacing as $10^4 S_0 = 0.91_{-0.37}^{+0.77}$ and $\langle D_0 \rangle = (87_{-11}^{+13})$ keV. The 18 roughly evenly distributed p levels in ^{40}Ar give $10^4 S_1 = 0.33_{-0.09}^{+0.14}$. The evaluations for S_0 , $\langle D_0 \rangle$, S_1 , and their statistical uncertainties are based on the method given in Ref. 24.

TABLE II. Resonance parameters of ^{40}Ar for $l=1$ levels.

E_0 (keV)	$g\Gamma_n$ (eV)	J
11.17 ± 0.01	0.14 ± 0.03	
17.95 ± 0.02	0.42 ± 0.07	
59.25 ± 0.05	5.9 ± 0.8	
115.7 ± 0.2	390 ± 50	$\frac{1}{2}$
180.4 ± 0.3	220 ± 50	
192.8 ± 0.3	90 ± 25	
274.7 ± 0.5	260 ± 80	
296.9 ± 0.6	300 ± 90	
301.1 ± 0.6	150 ± 50	
340.8 ± 0.7	720 ± 100	$\frac{3}{2}$
363.0 ± 0.8	105 ± 35	
371.3 ± 0.8	740 ± 160	
401.7 ± 0.9	410 ± 120	
455.4 ± 1.1	530 ± 140	
469.3 ± 1.1	1700 ± 400	$\frac{3}{2}$
531.6 ± 1.4	520 ± 150	
552.8 ± 1.4	300 ± 90	
569.3 ± 1.5	2700 ± 800	

We assume that the merged $g\Gamma_n^1$ population for the p levels having $J = \frac{1}{2}$ and $\frac{3}{2}$ follows a single channel Porter-Thomas (PT) distribution. Figure 3 shows the cumulative count of levels having $(g\Gamma_n^1)^{1/2}$ values larger than a given lower limit for the 18 p levels observed between 0 and 600 keV. Since about 5% of this energy interval would be blocked for observing p levels by the presence of the strong s levels, the effective energy interval is 570 keV. The three fit curves express the integral PT distributions of $(g\Gamma_n^1)^{1/2}$ values, with "A" normalized to $N=28$ and $10^4 S_1=0.25$, "B" normalized to $N=24$ and $10^4 S_1=0.35$, and "C" normalized to $N=20$ and $10^4 S_1=0.45$. Curve B uses a p strength function very close to the value determined independently as above, and gives a best fit to the experimental distribution. We thus obtained $\langle D_1 \rangle = (24 \pm 5)$ keV, where the uncertainties were estimated from curves A and C. This also implies that approximately six weak p levels with $g\Gamma_n^1 < 0.5$ eV were probably missed in the studied energy region. Considering the combined uncertainties of $\langle D_0 \rangle$ and $\langle D_1 \rangle$, it is consistent with the general prediction that $\langle D_0 \rangle \approx 3 \langle D_1 \rangle$ for zero target spin. Our single channel data show many small fluctuations in σ_t , which, in some cases, could be due to weaker p levels rather than to statistical fluctuations.

For the $l=0$ levels, the interference effects between net potential and resonance scattering are

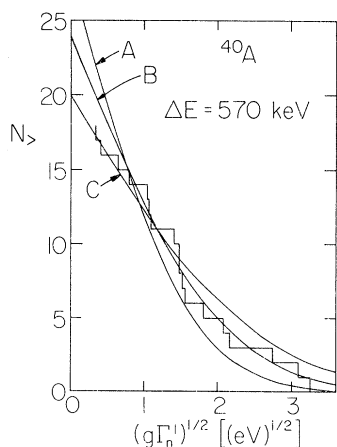


FIG. 3. Cumulative distribution of $(g\Gamma_n^1)^{1/2}$ values for the 18 observed p levels in ^{40}Ar . The effective energy interval ΔE is the observed interval (600 keV) minus the portions ($\sim 5\%$) blocked by the strong s levels. Three integral Porter-Thomas curves are plotted for comparison, with "A" normalized to $N=28$ and $10^4 S_1=0.25$, "B" normalized to $N=24$ and $10^4 S_1=0.35$, and "C" normalized to $N=20$ and $10^4 S_1=0.45$. Curve B gives the best fit, which leads to $\langle D_1 \rangle = (24 \pm 5)$ keV.

large. We tried R -matrix fits to these ^{40}Ar s levels, first treating one level at a time, and then by treating the four s levels between 150 and 270 keV simultaneously. The R -matrix curves have $\sigma_{\min} \approx 0$ on the low side of the resonances. The fits were poor until the correction was made for $\approx 5\%$ air in the samples, after which we obtain $\sigma \approx 0.7$ b/atom near 1 keV and $\sigma \approx 0$ at the minima where the net potential and resonance scattering amplitudes are nearly equal and opposite to each other.

For the R -matrix fit curve in Fig. 1(a), we have not included the contribution of the virtual level in ^{36}Ar which contributes ~ 0.25 b/atom to natural Ar near 1 keV. The fit to 150 keV uses $\Gamma_n = 5.6$ keV for a level at 76.2 keV, with a channel radius of 4.79 fm. We used $R^0 = A + B(E - E_{1/2})/E_{1/2}$ for other contributions⁶ to the R -matrix s scattering, with $A=0.6$, $B=0.13$, and $E_{1/2}=70$ keV. This gave $\sigma_{\text{pot}} = 0.34, 0.44, 0.54$, and 0.81 b/atom at 100, 76.2, 52.5, and 1 keV, respectively. The area analysis results have $\Gamma_n = 5.4$ keV, using $\sigma_{\text{pot}} = 0.47$ b/atom.

In Fig. 1(b), we chose for best fit, $\Gamma_n = 4.6, 1.8, 3.4$, and 0.53 keV, respectively, for levels at 171.7, 219.4, 254.3, and 267.6 keV, with $A = 0.65$, $B = 1.0$, and $E_{1/2} = 210$ keV. We obtain near zero measured σ_t values at the interference minima on the low side of all but the last s level at 267.6 keV. Our measured σ_t values are significantly above the R -matrix curves on the high energy sides of the four s levels in Fig. 1(b). This is partly due to some unresolved p levels.

Our resonance energies agree with those of Ref. 22 to within our combined energy uncertainties. For the $l=0$ levels our agreement is fairly good for the Γ values for the levels at 171.7, 219.4, and 254.3 keV, but poor for the other three levels. They give Γ values for each p level, but J values only for the levels at 455, 469 keV, and higher. For the levels for which they do not give J values, a comparison with our $g\Gamma_n$ values requires a choice of g . In all cases, our results are consistent within 40% for the best agreeing choice of g . Their experimental energy resolution was better than ours at the upper energies, but were progressively poorer than ours below ~ 200 keV. Their measured σ_t values in the region above the first strong s level shown in our Fig. 1(a) were in reasonable agreement with ours, and above our fit curve. They used a single sample having $(1/n) \approx 15$ b/atom.

We wish to thank Dr. H. Ceulemans, Dr. H. S. Camarda, Dr. M. Slagowitz, and Dr. S. Wynchank who made contributions in carrying out the measurements. The technical support by L. Morganstein, W. Van Wart, and the late A. Blake was also important for the success of the experiment.

*Research supported in part by the U.S. Atomic Energy Commission.

¹H. I. Liou *et al.*, Phys. Rev. C 5, 974 (1972), Er.

²F. Rahn *et al.*, Phys. Rev. C 6, 251 (1972), Sm, Eu.

³F. Rahn *et al.*, Phys. Rev. C 6, 1854 (1972), ²³²Th, ²³⁸U.

⁴H. I. Liou *et al.*, Phys. Rev. C 7, 823 (1973), Yb.

⁵H. S. Camarda *et al.*, Phys. Rev. C 8, 1813 (1973), W.

⁶F. Rahn *et al.*, Phys. Rev. C 8, 1827 (1973), Na.

⁷U. N. Singh *et al.*, Phys. Rev. C 8, 1833 (1973), K.

⁸H. I. Liou *et al.*, Phys. Rev. C 10, 709 (1974), Cd.

⁹G. Hacken *et al.*, Phys. Rev. C 10, 1910 (1974), In.

¹⁰F. Rahn *et al.*, Phys. Rev. C 10, 1904 (1974), Gd.

¹¹U. N. Singh *et al.*, Phys. Rev. C 10, 2143 (1974), Ca.

¹²U. N. Singh *et al.*, Phys. Rev. C 10, 2138 (1974), Cl.

¹³U. N. Singh, H. I. Liou, J. Rainwater, G. Hacken, and J. B. Garg, Phys. Rev. C 10, 2150 (1974), Mg.

¹⁴U. N. Singh, H. I. Liou, J. Rainwater, G. Hacken, and J. B. Garg, Phys. Rev. C 10, 2147 (1974), F.

¹⁵H. I. Liou *et al.*, following paper, Phys. Rev. C 11, 462 (1975), Dy.

¹⁶E. Melkonian, Phys. Rev. 76, 1750 (1949).

¹⁷R. E. Chrien, A. P. Jain, and H. Palevsky, Phys. Rev. 125, 275 (1962).

¹⁸D. G. Henshaw, Phys. Rev. 105, 976 (1957).

¹⁹V. E. Krohn and G. R. Ringo, Phys. Rev. 148, 1303 (1966).

²⁰G. E. McMurtrie and D. P. Crawford, Phys. Rev. 77, 840 (1950).

²¹*Resonance Parameters*, compiled by S. F. Mughabghab and D. I. Garber, Brookhaven National Laboratory Report No. BNL-325 (National Technical Information Service, Springfield, Virginia, 1973), 3rd ed., Vol. I.

²²F. T. Seibel, Ph.D. thesis, Duke University, 1968 (unpublished); private communication from Dr. E. G. Bilpuch and Dr. H. W. Newson.

²³*Neutron Cross Sections*, compiled by D. J. Hughes and R. B. Schwartz, Brookhaven National Laboratory Report No. BNL-325 (U.S. G.P.O., Washington, D.C., 1958), 2nd ed.

²⁴H. I. Liou and J. Rainwater, Phys. Rev. C 6, 435 (1972).